



ELSEVIER

Journal of Chromatography A, 717 (1995) 41–60

JOURNAL OF  
CHROMATOGRAPHY A

# Application of capillary electrophoresis, high-performance liquid chromatography, on-line electrospray mass spectrometry and matrix-assisted laser desorption ionization–time of flight mass spectrometry to the characterization of single-chain plasminogen activator

A. Apffel<sup>a,\*</sup>, J. Chakel<sup>a</sup>, S. Udiavar<sup>a</sup>, W.S. Hancock<sup>a</sup>, C. Souders<sup>b</sup>, E. Pungor Jr.<sup>b</sup>

<sup>a</sup>Hewlett-Packard Laboratories, MS26U/R6, 3500 Deer Creek Road, Palo Alto, CA 94304, USA

<sup>b</sup>Berlex Biosciences, 430 Valley Dr., Brisbane, CA 94005, USA

## Abstract

The analysis of recombinant *Desmodus* salivary plasminogen activator (DSPA $\alpha$ 1), a heterogeneous glycoprotein, is demonstrated through the use of high-performance liquid chromatography (HPLC), high-performance capillary electrophoresis (HPCE), liquid chromatography–electrospray mass spectrometry (LC–ES–MS), and matrix-assisted laser desorption ionization–time of flight mass spectrometry (MALDI–TOF–MS). The protein is analyzed at three specific levels of detail: the intact protein, proteolytic digests of the protein, and fractions from the proteolytic digest. A method for “on-column” collection of HPLC fractions for subsequent transfer and analysis by HPCE and MALDI–TOF–MS is shown.

## 1. Introduction

The development of rDNA-derived protein pharmaceuticals has been facilitated by the introduction of new analytical methods that can be used to characterize proteins and/or to demonstrate consistency of manufacture of a protein. Peptide mapping is a key method for monitoring the amino acid sequence and is able to detect small changes in small to moderate size proteins, e.g. insulin and human growth hormone. The analysis of a much larger protein, e.g. fibrinogen (molecular mass of 350 000), or the heterogeneous glycoproteins, such as antibodies (molecu-

lar mass of 150 000), is hindered by the complexity of the range of peptides generated by an enzymatic digestion. Such complexity makes a single reversed-phase high-performance liquid chromatography (HPLC) separation combined with on-line UV detection of limited utility.

The advent of commercially available combined HPLC and electrospray ionization mass spectrometry (LC–ES–MS) systems compatible with conventional HPLC methodology has increased the power of peptide mapping considerably [1,2]. LC–ES–MS in combination with in-source collisionally induced dissociation (CID) has been used effectively to identify sites of N- and O-linked glycosylation [3–5]. However, even this technique is limited by insufficient resolution

\* Corresponding author.

resulting from the large number of very similar peptides caused by variable protein glycosylation and enzymatic digests of moderately sized glycoproteins. It is therefore necessary to employ a range of techniques with orthogonal selectivity in order to characterize such samples. A significant issue is to efficiently utilize such multidimensional data in a way that multiple samples can be characterized for a product development program.

It is interesting to note the evolution of the terms “multidimensional” and “hyphenated”. Ten years ago, these terms were routinely used to mean the (generally) on-line coupling of two single-stage analytical instruments, such as chromatography and mass spectrometry. Now, however, such a coupling is widely accepted and the multidimensionality of the analysis is of a higher order. The power of recent techniques lies in utilizing chromatography, high-performance capillary electrophoresis (HPCE), UV-Vis, mass spectrometric, and other spectrometric data in an integrated manner.

We have, therefore, investigated the use of combinations of HPCE, HPLC, LC-ES-MS, and MALDI-TOF-MS to allow for characterization of enzymatic digests of underivatized glycoprotein samples. The separation selectivity of HPLC and CE is sufficiently orthogonal to yield a great deal of comparative information. Although LC-ES-MS is extremely powerful for peptide mapping, when dealing with intact proteins the mass range is limited to simple mixtures and lower-molecular-mass fragments compared with MALDI-TOF-MS. Thus in combining data from the two techniques, highly complementary data are obtained.

As an example of a heterogeneous glycoprotein, DSPA $\alpha$ 1, a single-chain plasminogen activator derived from *Desmodus rotundus* (vampire bat) salivary glands [6] was chosen. DSPA $\alpha$ 1 is a serine protease that plays a role in clot lysis. The potential applications for the molecule are in the area of thrombotic myocardial and cerebral infarctions, deep vein thrombosis, lung embolism, and peripheral arterial occlusive diseases. DSPA $\alpha$ 1 displays approximately 70% sequence homology with the double-chain serine

protease, tissue plasminogen activator (tPA), and may have a fibrin specificity, with a strict dependence on polymeric fibrin as a co-factor [7]. DSPA is known to be heterogeneous when expressed in CHO cells [8]. It is a large (441 amino acids) complex molecule of calculated (non-glycosylated) average molecular mass 49 508, with six sites for potential glycosylation, four O-linked and two N-linked. It has been proposed, based on homology with other serine proteases [6] that there are 28 cysteines forming 14 disulfide bridges.

## 2. Experimental

### 2.1. Instrumental

#### HPLC

The HPLC separation was performed on a Hewlett-Packard 1090 liquid chromatography system equipped with DR5 ternary solvent delivery system, diode-array UV-Vis detector, autosampler, and heated column compartment (Hewlett-Packard, Wilmington, DE, USA). All HPLC separations were done using a Vydac C<sub>18</sub> (Catalog No. 218TP54, Hesperia, CA, USA) 5- $\mu$ m particle, 300-Å pore size reversed-phase column. A standard solvent system of water (solvent A) and acetonitrile (solvent B), both with 0.1% trifluoroacetic acid (TFA), was used with a flow-rate of 0.2 ml/min. The gradient for the separation was constructed as 0–60% B in 90 min. The column temperature was maintained at 45°C throughout the separation.

A schematic for “on-column” fraction collection is shown in Fig. 1. The effluent from the HPLC (at 200  $\mu$ l/min) is mixed with a non-elutropic solvent, 0.1% TFA at 1000  $\mu$ l/min delivered with an Eldex Model A-30-S metering pump (Eldex Laboratories, Napa, CA, USA). The resultant mixture was selectively directed to one of four possible collection columns, or a bypass, using a Valco Model CST6UW 6-position, 14-port, electrically actuated valve (Valco Instrument, Houston, TX, USA). The collection columns consisted of HP hydrophobic sequencing cartridge columns (P.N. G1073A) in a col-

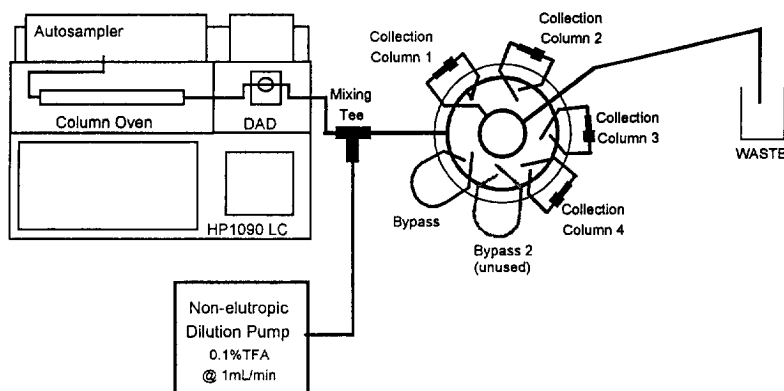


Fig. 1. Schematic of on-column fraction collection.

umn adapter (P.N. G1007A). Fractions were eluted from the collection columns using a gradient from 0 to 90% B in 5 min at a flow-rate of 0.2 ml/min and collected in Eppendorf vials. Four specific fractions were chosen to be collected from the endoproteinase ArgC digest of DSPA $\alpha$ 1. The fraction collection process was repeated for four separations with 250  $\mu$ l of sample at a concentration of 1.2 nmol/ml for a total sample consumption of 1.2 nmol. For each run, the specific fraction was directed to the appropriate cartridge. The samples were then eluted in approximately 200  $\mu$ l and concentrated to a final volume of 100  $\mu$ l. Thus approximately 1.2 nmol of each homogeneous peptide was collected while a lower amount is present for the heterogeneous glycoforms. Since in the original sample the 1.2 nmol was contained in 1000  $\mu$ l, while the final fraction volume was 100  $\mu$ l, an approximate ten-fold concentration was obtained along with isolation of the fractions.

#### High-performance capillary electrophoresis

HPCE was done on a Hewlett-Packard HP<sup>3D</sup>CE system with a built-in UV-Vis diode-array detector (DAD) and MS Windows Chemstation 3D software. A phosphate deactivated [9] fused-silica capillary of 50  $\mu$ m internal diameter and 56 cm effective length with a 150  $\mu$ m extended light path (bubble cell) (P.N. G1600-62232) was used. The capillary was thermostatted at 35°C. Before each separation, the capillary

was conditioned by flushing with 0.1 M NaOH for 2 min at 50 mbar, followed by flushing with background electrolyte for 5 min at 50 mbar. The background electrolyte consisted of 100 mM sodium phosphate buffer at pH 2.4 and 100 mM NaCl. Injections were made by pressure for 10–30 s at 50 mbar. For peptide separations, the injection was followed by a trailing electrolyte consisting of 1 mM phosphoric acid at 5 kV for 2 min. The use of this discontinuous buffer system served to sharpen the peaks from the injection plug. The separation was monitored at 200 and 280 nm.

#### Mass spectrometry

*LC-ES-MS.* Mass spectrometry was done on a Hewlett-Packard 5989B quadrupole mass spectrometer equipped with extended mass range, high-energy dynode detector (HED), and a Hewlett-Packard 59987A API-electrospray source with high-flow nebulizer option. Both the HPLC and MS were controlled by the HP Chemstation software, allowing simultaneous instrument control, data acquisition, and data analysis. The high-flow nebulizer was operated in a standard manner with N<sub>2</sub> as nebulizing (1.5 l/min) and drying (15 l/min at 300°C) gas.

To counteract the signal suppressing effects on LC-electrospray MS of trifluoroacetic acid, a previously reported method [10], referred to as the "TFA fix" was employed. The "TFA fix" consisted of post-column addition of propionic

acid-isopropanol (75:25) at a flow-rate of 100  $\mu\text{l}/\text{min}$ . The TFA fix was delivered using an HP 1050 HPLC pump and was mixed with a zero-dead-volume tee into the column effluent after the DAD detector and after the column-switching valve. Column effluent was diverted from the MS for the first 5 min of the chromatogram, during which time excess reagents and unretained components eluted.

For peptide mapping, MS data was acquired in scan mode, scanning from 200 to 1600 u at an acquisition rate of 1.35 Hz at 0.15 u step size. Unit resolution was maintained for all experiments. Data was filtered in the mass domain with a 0.03 u Gaussian mass filter and in the time domain with a 0.05 min Gaussian time filter. The fragment identification was done with the aid of HP G1048A protein and peptide analysis software, a software utility which assigns predicted fragments from a given sequence and digest with peak spectral characteristics.

For the in-source collisionally induced dissociation (CID) method for detecting fragments indicative of glycopeptides [3], the CapEx voltage was set to 200 V instead of the standard 100 V. Data acquisition was done in selected-ion monitoring (SIM) mode, monitoring ions at  $m/z$  147, 204, 292, and 366, each with a 1 u window and a dwell time of 150 ms, resulting in an acquisition rate of 1.5 Hz. Data was filtered in the time domain with a 0.05 min Gaussian time filter.

**MALDI-TOF-MS.** Mass spectra were generated with a Hewlett-Packard 1700XP (predecessor to the Hewlett-Packard G2025A) MALDI-TOF-MS system. This system utilizes a  $\text{N}_2$  laser (337 nm) for the desorption/ionization event coupled with a linear 1.7-m time-of-flight analyzer for mass analysis. Spectra were acquired at laser powers just above the ionization threshold using a matrix consisting of either 2,5-dimethoxy-4-hydroxycinnamic acid (sinapinic acid, HP P.N. G2055A) or 2,5-dihydroxybenzoic acid (DHBA, P.N. G2056A).

**Intact protein:** DSPA $\alpha$ 1 (0.55 mg/ml) was

mixed 1:1 with a 100 mM sinapinic acid matrix solution and two 1- $\mu\text{l}$  aliquots (ca. 10 pmol total) were sequentially deposited onto the probe tip and vacuum dried in the HP G2024A sample prep accessory. Data were collected at a 100 MHz sampling rate and a total of 100 laser shots were summed. The mass scale was calibrated using a protein standard mixture (HP P.N. G2053A) as an external calibrant.

**Protein digest mixture and HPLC pooled fractions:** The entire digest mixture sample was prepared by two different methods. For each method, data were collected at a 400 MHz sampling rate and a total of 100 laser shots were summed. The standard preparation method comprised of diluting the digest mixture (0.35 mg/ml) 1:9 with 100 mM sinapinic acid. Two 0.5- $\mu\text{l}$  aliquots (ca. 600 fmol total) were sequentially deposited onto the probe tip and vacuum dried. The alternative method involved generating a seed layer of polycrystalline DHBA on the probe tip and adding a sample-matrix solution to the bed of seed crystals [11]. In this technique, 1  $\mu\text{l}$  of a saturated DHBA matrix solution (30% acetonitrile) is added to the probe tip, allowed to air dry, and mechanically crushed with a glass slide. Non-adhering crystals were then brushed off of the probe tip. The digest mixture sample was diluted 1:9 with the supernatant of the saturated DHBA solution. Then 1  $\mu\text{l}$  of this solution (ca. 600 fmol) was applied to the bed of seed crystals where crystallization commenced immediately, allowed to sit for ca. 30 s, and rinsed with ca. 100  $\mu\text{l}$  water prior to the sample-matrix deposit completely drying out. This method offers an approach that greatly increases the tolerance to contaminants which may interfere in the crystallization process.

The HPLC fractions were mixed 1:1 with a 100 mM sinapinic acid and two 0.5- $\mu\text{l}$  aliquots were sequentially deposited onto the probe tip and vacuum dried. Data were collected at a 400 MHz sampling rate and a total of 75 laser shots were summed for each fraction.

The mass scale was calibrated using a peptide standard mixture (HP P.N. G2052A) as an external calibrant.

## 2.2. Chemicals and reagents

HPLC-grade acetonitrile and trifluoroacetic acid (TFA), as well as EDTA were obtained from J.T. Baker (J.T. Baker, Phillipsburg, NJ, USA). Distilled, deionized Milli-Q water (Millipore, Bedford, MA, USA) was used. Urea was obtained from GIBCO (Gaithersburg, MD, USA), D,L-dithiothreitol (DTT), iodoacetic acid, bicine, NaOH, and CaCl<sub>2</sub> were obtained from Sigma (Sigma, St. Louis, MO, USA). The enzyme endoproteinase Arg-C (Boehringer Mannheim, Indianapolis, IN, USA) was used for mapping. Recombinant DSPA $\alpha$ 1 (from Berlex Biosciences, Richmond, CA, USA) was purified from CHO cells, and the starting concentration was 0.55 mg/ml.

## 2.3. Methods

### Sample preparation

DSPA $\alpha$ 1 (5 mg) was denatured in 6 M urea and titrated with 5 M NaOH to pH 8.3. The sample was then reduced using 32 mM DTT (molar excess to DSPA 1:300) by incubating at 55°C for 3 h. Alkylation of the reduced protein was done by a further 30 min incubation with 70 mM iodoacetic acid. The reduced and alkylated DSPA $\alpha$ 1 was then desalted using size-exclusion chromatography.

### Arg-C digestion

The reduced, alkylated, desalted DSPA $\alpha$ 1 was digested in 200 mM bicine at 37°C with an enzyme-to-substrate (mass) ratio of 1:50 for 18 h in the presence of 20 mM DTT, 0.5 mM EDTA, and 8.5 mM CaCl<sub>2</sub>. The digestion was quenched by titrating the sample to pH 1.5.

## 3. Results and discussion

### 3.1. Analytical strategy

The analytical approach used for the analysis of the DSPA $\alpha$ 1 glycoprotein was to start at the gross level of the intact protein and use ana-

lytical techniques applicable to such a complex, high-molecular-mass sample. Following this characterization, the greater detail of the peptide map from an endoproteinase Arg-C digest was examined, followed by individual fractions from the digest. Thus the focus moved from more global properties of the sample to increasing degrees of detail. At each level, HPLC, LC-MS, HPCE, and MALDI-TOF-MS were applied. At the more global level, it is not possible to discern the detailed information of the specialized techniques. On the other hand, it is difficult to synthesize data from the more specific into a more global picture. This problem of context of scale of macromolecular analysis is at the heart of the need for multidimensional analysis. With samples of this complexity, no one technique yields the required depth of structure information combined with ready linkage to the overall structure of the macromolecule.

### The intact glycoprotein

At the level of detail of the intact glycoprotein, information can be gathered concerning the gross chemical and structural characteristics of the protein as well as the purity of the sample preparation. In the current study, the DSPA $\alpha$ 1 sample had already undergone a number of purification steps to isolate it from the cells in which it was cultured. With such a protein, there exist multiple opportunities for heterogeneity, including glycosylation, varying N-terminal sequence, amino acid modifications, and proteolytic clipping. The goal of the purification step for a recombinant DNA derived pharmaceutical glycoprotein such as DSPA $\alpha$ 1 is to be combined with the production process to produce a high-purity product in a consistent manner. Such a product, however, may still contain substantial heterogeneity introduced by post-translational modifications such as glycosylation. Therefore, the analytical sample may consist of a mixture of not only potential contaminants, but heterogeneous glycoforms as well, which are an intrinsic part of the target molecule. It is the challenge of the analytical chemist to devise a suitable set of methods that

can be applied to such complex samples. Of course, in addition to separation methods discussed below, a wide range of tools including N- and C-terminal sequence analysis, X-ray crystallography, and biological activity tests can be applied.

The initial examination of the intact protein sample was performed by reversed-phase HPLC and is shown in Fig. 2. From the separation, it can be seen that the sample is quite pure, and at least in terms of hydrophobicity, relatively homogeneous, although product variants may not be separated under the applied conditions [12]. Through the use of UV-Vis diode-array detection, its UV spectra can be acquired throughout the separation (see Fig. 2, inset) and data can be obtained concerning the relative number of aromatic amino acids (tryptophan, tyrosine, and phenylalanine) present in the protein. In those cases for which the amino acid composition is known, this information can also be used as a partial identification for the peak in the presence of other proteins.

The capillary electrophoresis separation (see Fig. 3) is used to characterize the intact protein as well as to gather UV-Vis spectral information. In addition, the orthogonality of the separation mechanism, being based on charge rather than hydrophobicity, is useful in the further

characterization of purity and homogeneity. In the case of a glycoprotein such as DSPA $\alpha$ 1, the charge heterogeneity introduced from the variable sialic acid content due to the glycosylation results in a relatively broad peak, but the absence of other well-separated peaks is consistent with low levels of other contaminating proteins.

The analysis of the intact glycoprotein by MALDI-TOF-MS (shown in Fig. 4) yields information similar to that of HPCE. Although often a destructive technique, the separation is based on mass/charge, as is electrophoresis. Strictly speaking HPCE is based on size/charge, but for denatured peptides this is closely related to mass. The two major peaks in the spectrum represent singly and doubly charged ions from the protein. The mass of the protein, determined from the singly charged ion, is  $54\,111.6 \pm 54$  compared with the average molecular mass of 49 508.15 calculated from the amino acid sequence only. The difference in  $M_r$  of 4603 or approximately 9.3% indicates a mass increase due to glycosylation. The peak width of approximately  $M_r$  5000 is related to the degree of microheterogeneity of glycosylation. Based on the expected resolution of the MALDI-TOF-MS experiment, if DSPA $\alpha$ 1 were homogeneous, it would have a peak width at half height on the order of  $M_r$  500 due, in part, to the isotopic

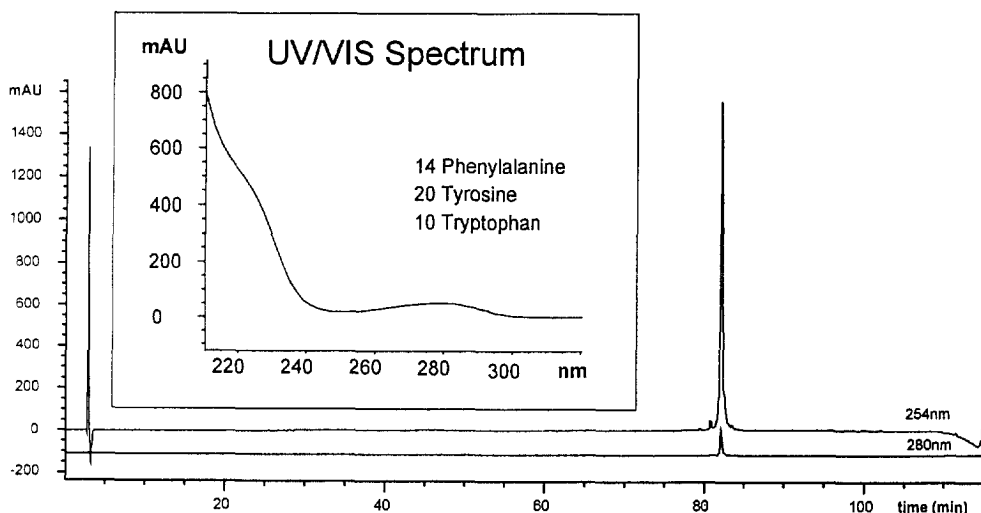


Fig. 2. HPLC of intact protein; 20  $\mu$ g total protein injected. See text for conditions.

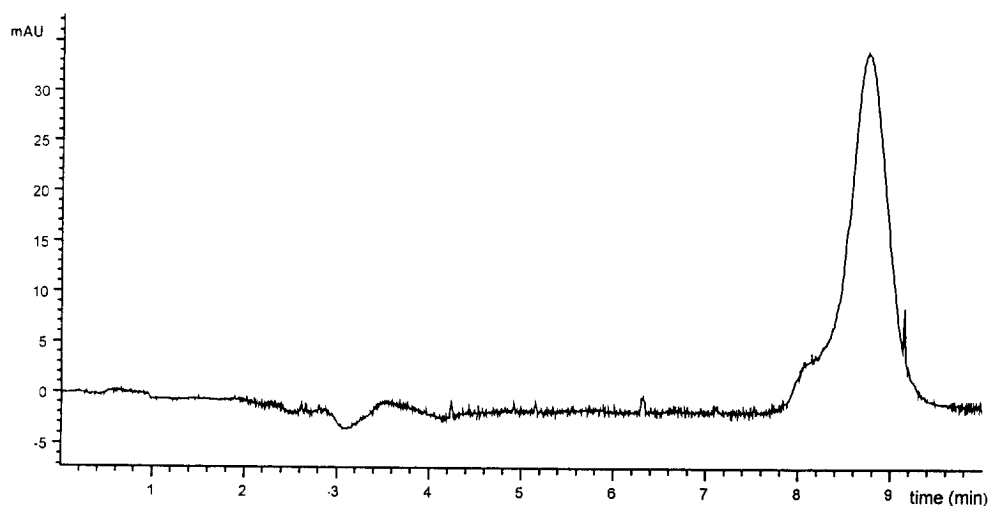


Fig. 3. CE of intact protein; 40 pmol total protein injected. See text for conditions.

distribution. In addition, there is some fine-structure of the  $[M+1]^+$  peak, which may indicate the presence of heterogeneous glycoforms.

It is useful at this level, as well as other levels of detail, to compare the relative sensitivity of the three techniques discussed above. In the case of HPLC, the total amount of sample applied was 20  $\mu\text{g}$  injected in a volume of 10  $\mu\text{l}$ , or a sample concentration of 2 mg/ml (40 mmol/ml). As can be seen from the chromatogram, the HPLC separation could be run at significantly

lower concentration. In the case of the HPCE separation, a pressure injection of 1500 mbar s (50 mbar  $\times$  30 s) resulted in an injection volume of 10 nl, of an original sample concentration of 0.51 mg/ml, corresponding to 5 pg. While the mass sensitivity of HPCE is very good, due to the low injection volumes and short detection path lengths, the absolute concentration sensitivity is less impressive. In the case of MALDI-TOF-MS, a relatively small amount of sample is applied. The sensitivity is even more impressive

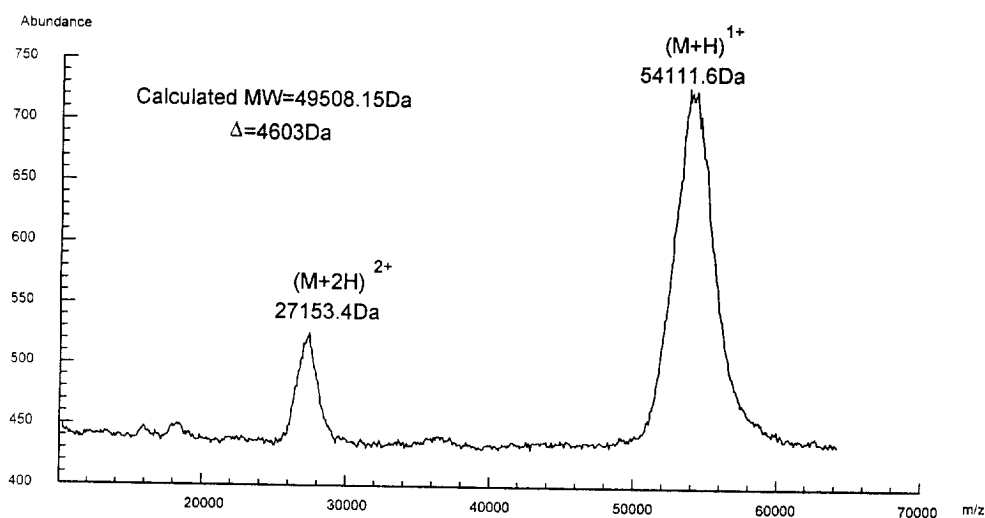


Fig. 4. MALDI-TOF-MS of intact protein; 10 pmol total protein applied. Matrix: sinapinic acid.

when one considers that of the 10 pmol applied, probably less than 100 fmol are consumed. The MALDI-TOF-MS technique generates useful data even when only 10–100 fmol of sample are applied.

#### The proteolytic digest

At the next level of detail, the intact glycoprotein is digested through the use of a proteolytic enzyme, resulting in a mixture of not only fragments due to the selectivity of cleavage, but of different glycoforms of specific glycosylated fragments as well. If, as is the case for DSPA $\alpha$ 1, the cDNA sequence of the protein is known, the peptide map generated by the separation of the digest can be compared with the predicted sequence.

The generation of peptide maps through the chromatographic or electrophoretic separation of the proteolytic digest (as shown in Fig. 5) is extremely powerful in generating a “fingerprint” of the protein. However, when the separation is monitored with a UV-Vis detector, complete

identification of the individual fragments is problematic. Although it has been shown that the individual fragments can be identified by comparing the UV spectra with those of standards, fragment identification usually requires fraction collection and subsequent analysis by mass spectrometry or N-terminal peptide sequencing.

The orthogonal separation mechanisms of reversed-phase HPLC and HPCE are evident in comparing the elution patterns of the two separations shown in Fig. 5. This can be exploited to resolve areas in one mode which co-elute in the other. The orthogonality of the separation mechanisms can also be used in a quality control environment as a fingerprint which can detect subtle changes in the protein product.

MALDI-TOF-MS can also be used to characterize enzymatic digest, as shown in Fig. 6. In this complex spectrum, a number of the predicted fragments can readily be identified. However, it is not possible to identify all the digest fragments present in the sample, due to a number of factors. The lack of chromatographic or

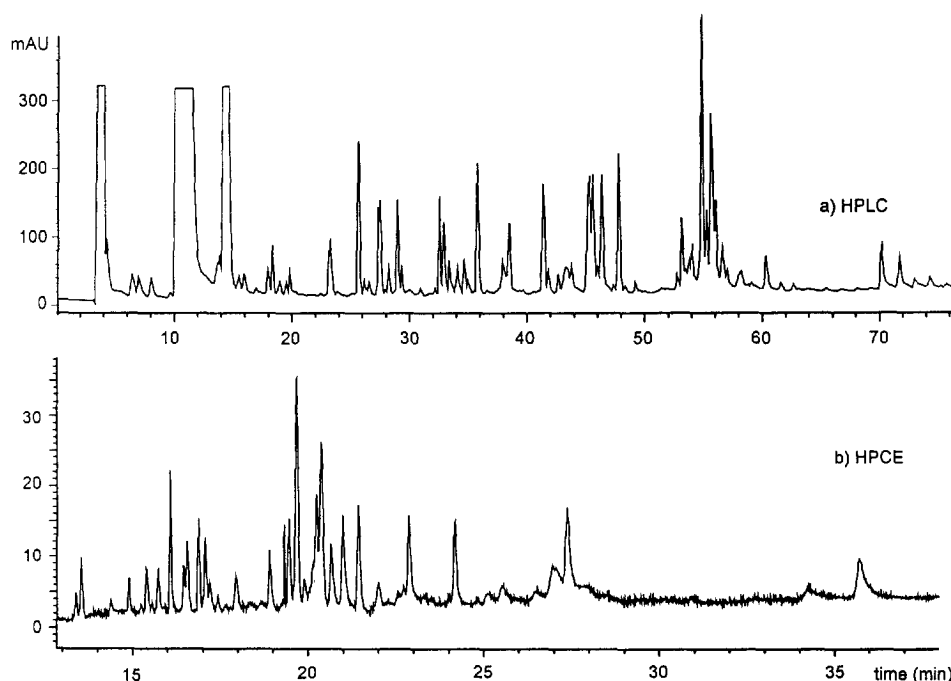


Fig. 5. HPLC and CE of digest. (a) HPLC monitored at 214 nm; 78 pmol injected. (b) HPCE monitored at 200 nm; 5 pmol applied. See text for other conditions.



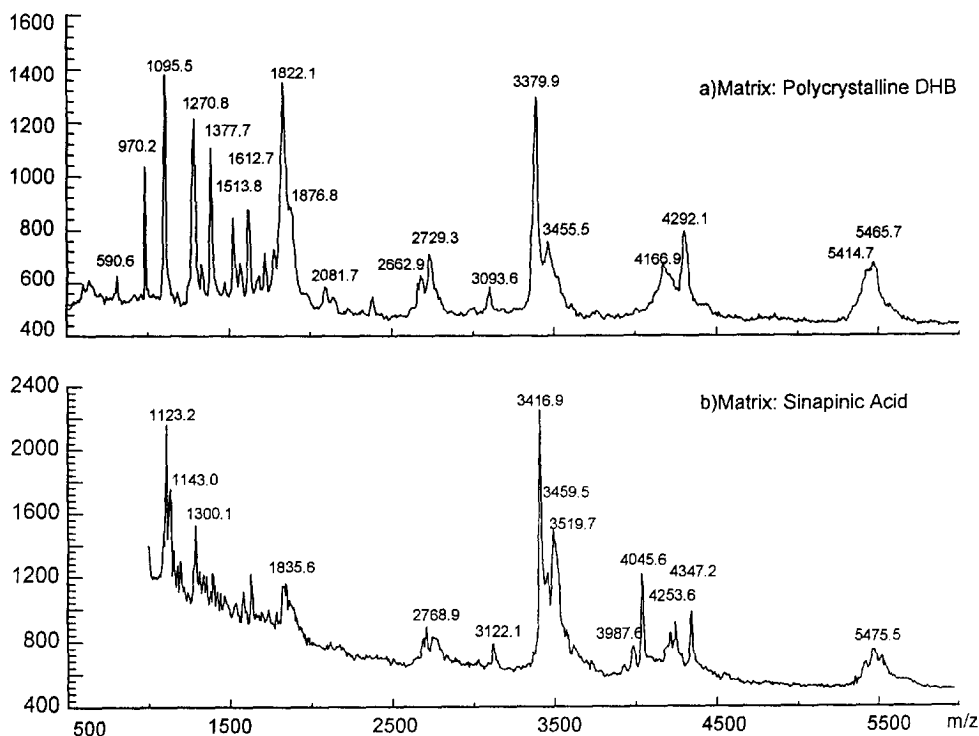


Fig. 6. MALDI-TOF-MS of digest; 500 fmol total protein applied. (a) Matrix: polycrystalline DHBA, (b) sinapinic acid.

electrophoretic separation hinders the ability to spot glycopeptides in complex mixtures. Furthermore, isobaric peptides cannot be resolved by mass spectrometric techniques alone. The complexity of the sample introduces selectivity in the ionization process which may suppress specific fragments. Often, 60–80% of the expected digest fragments are observed. The formation of matrix adducts may further complicate the mixture and may result in ions which are difficult to identify. In the lower mass range, matrix background ions are also present. For specific applications, selectivity can be optimized by judicious choice of matrix. In the data shown in Fig. 6, better detail is obtained in the lower mass range through the use of polycrystalline dihydroxybenzoic acid (DHBA) as a matrix than sinapinic acid. In general, lower-molecular-mass peptides (<2000) have higher desorption/ionization yields with DHBA than with sinapinic acid. More extensive coverage of a digest mixture can be realized via MALDI-TOF-MS analysis of pre-fractionated HPLC pools of the mixture. Even though the

single-dimensional analysis via MALDI-TOF-MS of enzyme digests is generally not comprehensive, it can be used to quickly generate a characteristic fingerprint similar to HPLC and HPCE.

The on-line combination of HPLC and electrospray ionization mass spectrometry adds a dimension to the analysis of peptide maps which makes it possible to identify most, if not all, of the predicted fragments. The LC-ES-MS analysis of the endoproteinase Arg-C digest of DSPA $\alpha$ 1 is shown in Fig. 7. The UV signal at 220 nm is shown in the lower half of Fig. 7 for comparison. Note that the sensitivities of the two detectors (UV and MS) are similar and that most peaks show up in both traces, although the individual intensities may differ.

Electrospray ionization is particularly useful in the identification of relatively high-molecular-mass peptides because of its ability to generate a set of multiply charged ions [13] which can be used to determine the molecular mass of the peptide even when the molecular mass is far in

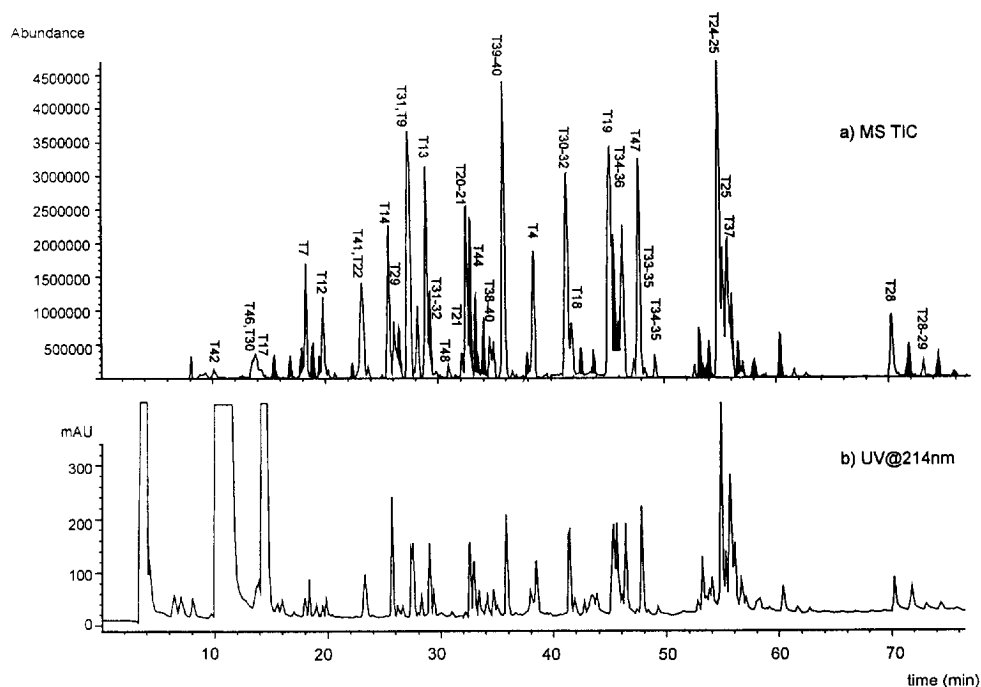


Fig. 7. LC-MS of digest; 78 pmol total protein injected. (a) Mass spectrometry total ion current, (b) 214 nm.

excess of the range available to the mass analyzer for singly charged molecules. For peptides found in enzymatic digests, molecular masses are typically below 5000 and the charge states are typically less than +5 (positive ion mode). The mass accuracy of the determination is typically better than 0.02%. In these experiments, mass spectral resolution was maintained at unit resolution across the scanned mass range and the sample was based on 78 pmol total protein. This is an important aid in assigning charge states to ions from peptides.

The identified fragments are listed in Table 1. The peaks which are unidentified are highlighted in Fig. 7. The interpretation of the peptide map was aided through the use of a software interpretation utility which greatly facilitates assignment of the predicted fragments to specific peaks in map. The software can also suggest anomalous sub-sequence fragments and modifications.

Although endoproteinase Arg-C was used as the proteolytic enzyme, there were a number of fragments which could not be explained by the cleavage selectivity of this enzyme. However,

most of the fragments could be accurately assigned as fragments produced by a tryptic digest. Trypsin cleaves peptide bonds on the C-terminal side of arginine or lysine residues. By contrast, endoproteinase Arg-C selectively cleaves only after arginine residues and, as such, the peptide fragment mixture which is generated by Arg-C can be considered a subset of a tryptic digest. All Arg-C fragments can be interpreted as single or multiple tryptic fragments. Future studies on DSPA $\alpha$ 1 will use preparations of the endoproteinase that show a greater degree of arginine specificity.

Table 2 shows a list of predicted fragments which were not identified in the LC-ES-MS analysis. A number of predicted fragments were not identified because the mass of the singly charged ions falls below the scanned molecular-mass range (200–1800). Interestingly, those digest fragments which are expected to be glycosylated (O-linked: T25, T36, T39, T45; N-linked: T15, T43) are either missing or are found at low abundance relative to other fragments, and can be used as a rough predictor of glycosylation

Table 1  
Found fragments

Retention time	Deconvoluted mass	Explanation
10.20	[475.2]	Fragment 42 (355–358) CAPK
13.57	[877.9]	Fragment 46 (420–427) DVPGV YTK
	[439.4]	Fragment 30 (254–256) TYR
18.29	[1104.4]	Fragment 7 (31–38) VEHCQ CDR
19.46	[1260.5]	Combination of fragments 6 to 7 (30–38) RVEHC OCCR
19.77	[780.3]	Fragment 12 (84–89) CEVDT R
23.25	[721.4]	Fragment 41 (349–354) LYPSS R
23.25	[677.3]	Fragment 22 (176–181) ATCGL R
25.59	[993.5]	Fragment 14 (102–110) GTWST AESR
26.52	[542.4]	Fragment 22 9249–253) VVLGR
28.89	[1404.6]	Fragment 13 (90–101) ATCYE GQGVT YR
29.86	[1520.2]	Combination of fragments 31 to 32 (257–267) VKPGE EEQTF KVK
30.91	[628.3]	Fragment 48 (437–441) DNMHL
32.11	[1488.6]	Fragment 21 (163–175) FTSES CSVPV CSK
32.84	[2440.1]	Combination of fragments 20 to 22 (163–181) AGKFT SESCS VPVCS KATCG LR
34.05	[1452.6]	Fragment 44 (364–376) TVTNN MLCAG DTR
35.75	[2151.1]	Combination of fragments 38 to 40 (283–348) HKSSS PFYSE QLKEG HVR
36.91	[1867.9]	Combination of fragments 39 to 40 (333–348) SSSPF YSEQL KEGHV R
38.44	[1298.7]	Fragment 4 (18–27) QESWL RPEVR
41.34	[1938.0]	Combination of fragments 30 to 32 (254–269) TYRVK PGEEE QTFKV K
41.82	[1879.8]	Fragment 18 (130–145) MPDAF NLGLG NHNYC R
45.21	[1645.9]	Fragment 19 (146–159) NPNGA PKPWC YVIK
46.31	[4216.1]	Combination of fragments 34–36 (271–306) YIVHK EFDDD TYNND IALLQ LKSDS PQCAQ ESDSV R
47.76	[1120.6]	Fragment 47 (428–436) VTNYL GWIR
48.31	[2795.4]	Combination of fragments 33 to 35 (270–292) KYIVH KEFDD DTYNND DIALL QLK
49.22	[2667.3]	Combination of fragments 34 to 35 (271–292) YIVHK EFDDD TYNND IALLQ LK
54.79	[3414.6]	Combination of fragment 24 to 25 (183–212) YKEPQ LHSTG GLFTD ITSHP WQAAI FAQNR
55.23	[3123.5]	Fragment 25 (185–212) EPQLH STGGL FTDIT SHPWQ AAIFA QNR
55.62	[2767.1]	Fragment 37 (307–330) AICLP EANLQ LDPWT ECELS GYGK
70.21	[3517.6]	Fragment 28 (219–248) FLCGG ILISS CWVLT AAHCF QESYL PDQLK
73.09	[4041.9]	Combination of fragments 28 to 29 (219–253) FLCGG ILISS CWVLT AAHCF QESYL PDQLK VVLGR

sites. This pattern was consistent with carbohydrate characterization studies [14] performed by others. There are also a number of lower-abundance fragments which were not identified at this stage, but based on previous studies it would be expected that secondary cleavages induced by the protease are the cause of many such fragments.

The characterization of enzymatic digests of glycoproteins by LC–ES–MS can be approached in three ways [15]. If the mass spectral data is presented as a contour map of  $m/z$  versus time

versus intensity, series of unresolved glycopeptides will appear as diagonal bands, since for a given digest fragment, glycoforms with a greater degree of glycosylation will appear as slightly heavier and elute somewhat early [1]. A second method consists of using in-source collisionally induced dissociation to fragment glycopeptides, producing marker ions indicative of specific types of glycosylation [3]. Finally, if the sequence of the protein is known, fragments and their glycoforms can be predicted from knowledge of typical glycosylation patterns. One can then hunt for

Table 2  
Not found fragments

Fragment	<i>m/z</i>	Sequence	Reason
T2[8–16]	1155.5	DEITQ MTYR	?
T3[17]	174.1	R	Low mass
T5[28–29]	233.1	SK	Low mass
T6[30]	174.1	R	Low mass
T8[31–38]	430.2	GQAR	?
T10[56–82]	3185.2	CHTVP VNCS EPR	?
T11[38]	174.1	R	Low mass
T15[111–123]	1591.8	VEGIN WNSL LTR	Possible N-linked glycosylation
T16[124]	174.1	R	Low mass
T23[182]	146.1	K	Low mass
T26[213]	174.1	R	Low mass
T27[214–218]	534.2	SSGER	?
T33[270]	146.1	K	Low mass
T43[349–363]	667.4	FLFNK	Possible N-linked glycosylation
T45[377–419]	4649.0	SGEIV PNVHD ACQGD SGGPL	Possible O-linked glycosylation
		VCMND NHMTL LGIIS WGVGC	
		GEK	

the specific glycoforms through the use of extracted ion chromatograms [16].

In this study, specific N-linked glycosylation was identified in DSPA $\alpha$ 1. The possible sites of N-linked glycosylation can be identified from the known sequence by the consensus sequence Asn–X–Ser(Thr). The N-linked structure is connected to the Asn residue. In DSPA $\alpha$ 1, the two possible N-linked sites are at residue 117 in fragment T15[111–123] and residue 362 in fragment T43[359–363]. N-linked glycopeptides generated in mammalian cell lines often fall into three general classes: high-mannose, complex, and hybrid. The expected glycosylation patterns in DSPA $\alpha$ 1 include high-mannose and complex structures, as illustrated in Fig. 8. All of these structures share the GlcNAc<sub>2</sub>Man<sub>3</sub> backbone structure shown in the outlined triangle. The heterogeneity is introduced by the number of mannoses in high-mannose structures and the degree of branching in the complex structures. Branching in complex structures can be introduced by the HexNAc + Hex structure in the outlined rectangle. Further microheterogeneity can be introduced by the addition of fucose or sialic acid.

The choice of the proteolytic enzyme is im-

portant in the characterization of glycoproteins. The enzyme is typically chosen such that there is only one possible glycosylation site per fragment, as is the case for Arg-C digest of DSPA $\alpha$ 1. Fortunately, the unexpected additional fragmentation encountered maintained this selectivity.

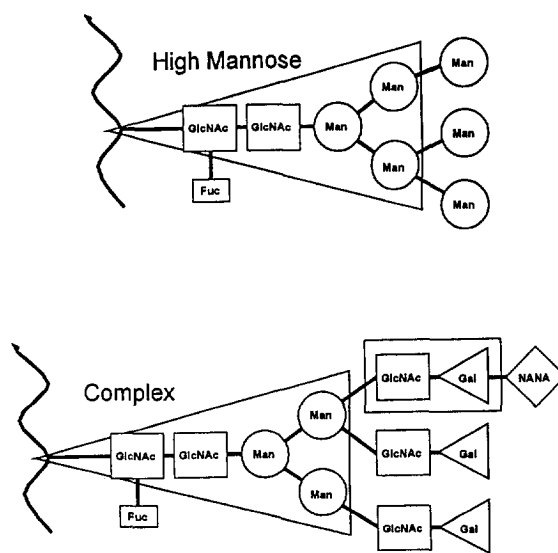


Fig. 8. Schematic of N-linked glycoforms.

Although the use of contour maps has been shown to be of utility in locating sites of glycosylation [2], the success of such an approach depends largely on the complexity of the glycosylation and the sensitivity of LC–MS analysis. If the sample is very heterogeneous, it will be difficult to differentiate the characteristic diagonal pattern from background signals. Fig. 9 shows a contour for a section of the Arg-C map of DSPA $\alpha$ 1 from 40 to 50 min. The encircled area shows signal due to fragment T15[111–123] complex sialylated biantennary structures with two different charge states (+2 and +3) for different degrees of sialylation. Although the characteristic pattern is evident in this figure, in point of fact, these glycopeptides were identified through the use of extracted ions, as described below.

The use of in-source collisionally induced dissociation in the analysis of DSPA $\alpha$ 1 is illustrated in Fig. 10. The CID mass spectral acquisition was carried out in selected-ion monitoring (SIM) mode to increase the sensitivity. The marker ions which were monitored are shown in Table 3. The reproducibility of the HPLC separation is sufficiently good that areas identified in the SIM analysis can be accurately

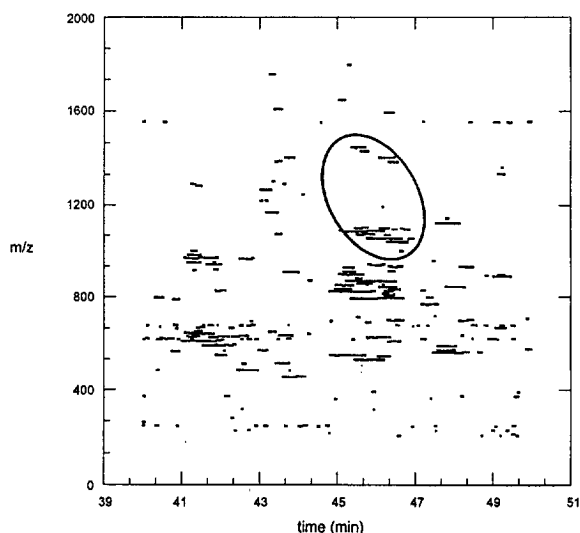


Fig. 9. Detail of contour map for DSPA $\alpha$ 1 Arg-C digest; 78 pmol total protein injected. CapEx voltage = 100 V. Data for signal >2000 counts shown.

compared with separate full spectral acquisitions conducted at lower fragmentation energy. This allows the parent glycopeptide to be identified. The success of this technique is limited by the complexity of the original glycoprotein and the sensitivity of the LC–MS system. In cases where there is a large degree of microheterogeneity due to glycosylation, there may not be an sufficient amount of an individual glycopeptide present to generate an interpretable low-energy spectrum. Note, however, that the sensitivity from the SIM CID data is sufficient since all of the different chromatographically unresolved glycoforms will contribute fragment ions to the electrospray signal. The summation of the signals due to the marker ions results in relatively broad looking chromatographic peaks. Based on the CID data, it is possible to infer some glycostructure differentiation. For example, all N-linked structures will generate a  $m/z$  204 ion corresponding to the HexNAc in the backbone structure. All complex N-linked glycopeptides will generate a  $m/z$  366 ion corresponding to the HexNAc + Hex structure indicative of the branching in multi-antennary structures. Only fucosylated glycopeptides will generate  $m/z$  147 and only sialylated glycopeptides will generate a  $m/z$  292 ion.

If the sequence is known and the glycosylation pattern of the host cell line is known, glycopeptides can be predicted and searched for in full scan mass spectral data via extracted ions. Individual glycopeptides which are present in such low amounts as to not generate an appreciable signal in the total ion current may be identified much more sensitively by looking only at the signals due to specific ions. An example is shown in Fig. 11, in which extracted ions corresponding to the T15 complex biantennary structure with different numbers of sialic acid are shown. Note that the region between 43.0 and 43.5 shows essentially no peaks in the total ion current. This is because the individual glycopeptides are present at significantly lower levels than a homogeneous non-glycosylated peptide fragment. From previous carbohydrate analysis, is known that DSPA $\alpha$ 1 glycosylation is approximately 34.5%

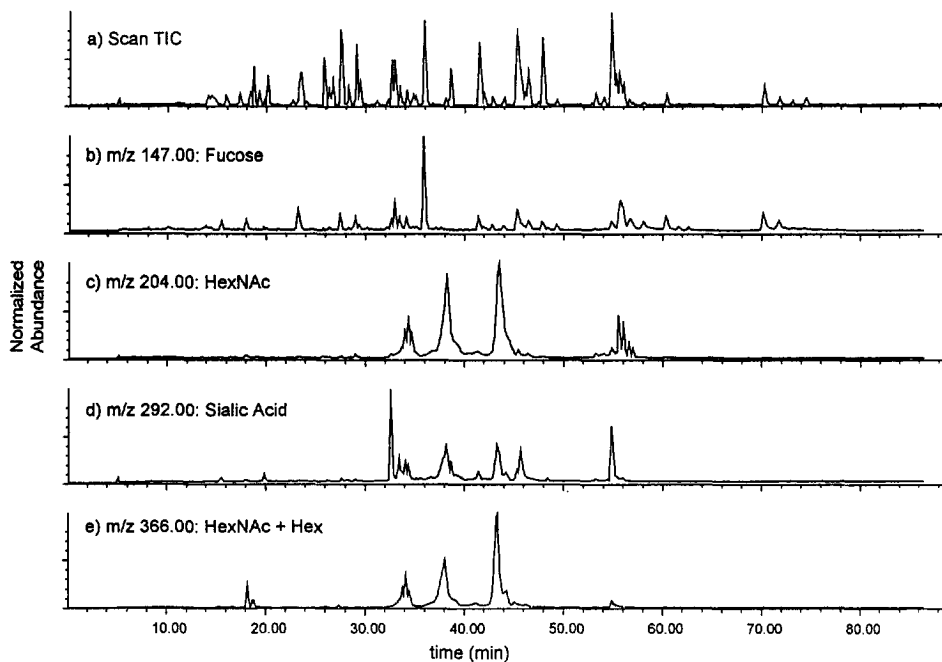


Fig. 10. CID detection of glycopeptides; 78 pmol total protein injected. (a) Total-ion chromatogram from scan acquisition (CapEx = 100 V), (b)–(e) from selected-ion monitoring acquisition (CapEx = 200 V): (b)  $m/z$  147, (c)  $m/z$  204, (d)  $m/z$  292, (e)  $m/z$  366 relative molecular mass.

high-mannose, 39.2% biantennary sialylated, 18.2% biantennary asialylated, 7.1% triantennary, and 1.1% tetraantennary [14]. In future work, in order to detect more of these structures, it will be necessary to utilize further preconcentration to improve the detection limits of the technique.

#### HPLC fractionation of the digest

In many cases, the complexity of the mixture generated by an enzymatic digest of a glycoprotein is too high for all components to be com-

pletely resolved by a single-dimensional analytical technique. Even two-dimensional techniques such as (LC or CE)–DAD UV–Vis or LC–MS have insufficient separation power to completely resolve the mixture. In these cases, an orthogonal third dimension can be exploited. While three-dimensional systems have been employed on-line [17], we chose to transfer samples from an LC separation to subsequent analysis in a semi off-line technique. Fractions eluting from the reversed-phase HPLC separation were selectively transferred onto disposable hydrophobic collec-

Table 3  
Glycomarkers

Sugar	Symbol	Chemical formula	Mass	Ion monitored [M + 1] <sup>+</sup>
Fucose	Fuc	C <sub>6</sub> O <sub>5</sub> H <sub>13</sub>	146.1	147.1
Hexose	Hex	C <sub>6</sub> O <sub>6</sub> H <sub>12</sub>	162.1	163.1
N-Acetylhexosamine	HexNAc	C <sub>8</sub> O <sub>6</sub> NH <sub>15</sub>	203.2	204.2
N-Acetylneuraminic acid	NANA	C <sub>11</sub> O <sub>9</sub> NH <sub>19</sub>	291.3	292.1
Complex branch unit	HexNAc + Hex		365.3	366.3

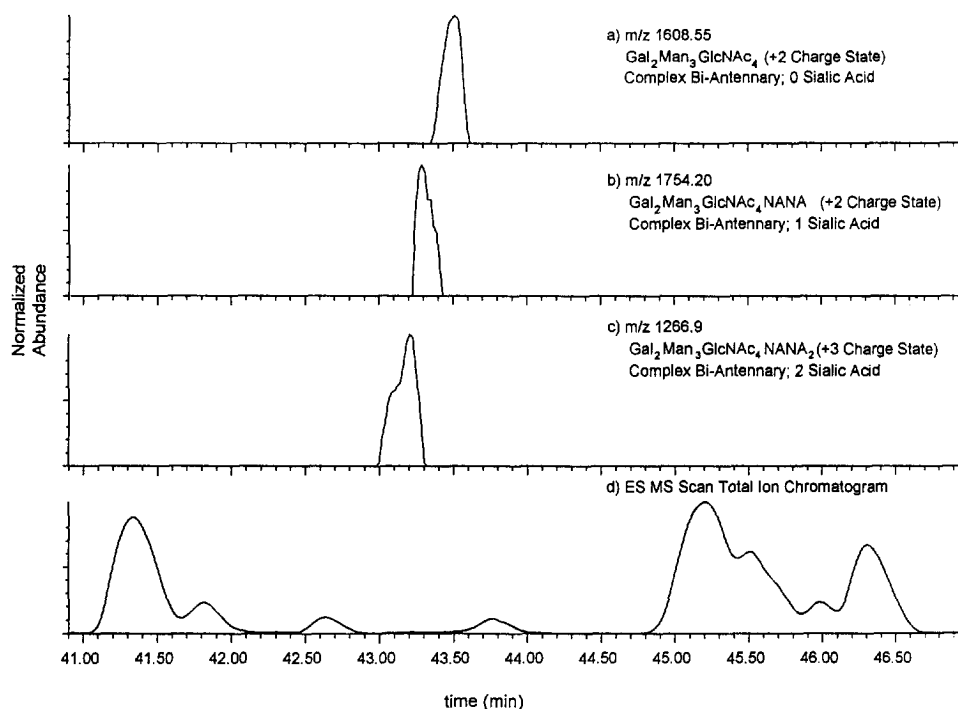


Fig. 11. Extracted ion detection of glycopeptides. Scan acquisition (CapEx = 100 V). (a) Extracted  $m/z$  1608.55,  $\text{Gal}_2\text{Man}_3\text{GlcNAc}_4\text{NANA}_0$  (+2 charge state). (b) Extracted  $m/z$  1754.2,  $\text{Gal}_2\text{Man}_3\text{GlcNAc}_4\text{NANA}_1$  (+2 charge state). (c) Extracted  $m/z$  1266.9,  $\text{Gal}_2\text{Man}_3\text{GlcNAc}_4\text{NANA}_2$  (+3 charge state). (d) Total-ion chromatogram.

tion columns after the effluent was diluted with a non-elutropic solvent. Because of the highly reproducible retention times of the LC separation, this process could be repeated, loading fractions from multiple LC runs on single collection columns. The hardware setup employed used a 14-port, 6-position valve which would allow four collection columns to be randomly accessed in addition to a bypass path. Following fraction collection, the fractions were eluted from the collection column with a rapid gradient. Since the fraction elution solvent does not have to be the same as the solvent system used in the peptide map, buffer transfer or desalting can also be accomplished in this step. This had the advantages of concentrating the samples for subsequent analysis and of great flexibility in transferring the sample fraction to subsequent analytical techniques.

This technique is particularly useful in transferring samples to subsequent HPCE separation.

As mentioned above, HPCE suffers from rather poor concentration sensitivity due to relatively small injection volumes and short-path-length UV detection. While on-line sample focusing and preconcentration techniques such as sample stacking [18] and capillary isotachopheresis (CITP) [19,20] are extremely useful in this respect, the low concentration of individual glycopeptides requires additional concentration to fully characterize the sample.

The technique is also useful for transferring samples to inherently static techniques such as MALDI-TOF-MS, in which an on-line flow-based approach would be difficult. The fractionation step itself is very important in reducing the complexity of the mixture to a point at which most of the components can be identified mass spectrally by MALDI-TOF-MS. The desalting characteristics of the fraction elution step can be very useful in increasing signal yields and the fraction of components observed.

Four fractions were collected from the HPLC peptide map, as illustrated in Fig. 12. Fractions 1 and 2 were chosen because of the high degree of glycosylation present in these areas as shown by the CID studies on glycomarkers. Fractions 3 and 4 were chosen because of the absence of glycoforms and because they represent fairly clean subsets of the entire map for subsequent evaluation. The benefits of the approach are not only the simplification of the analytical sample via fractionation, but a concentration step of approximately ten-fold as well.

The four fractions were analyzed by HPCE using the same method as had been used for the total digest. The electropherograms of the four fractions and the original digest are shown in Fig. 13. Referring to the HPLC fractions shown in Fig. 12, it can be seen that the first three HPLC fractions agree with this figure reasonably well in terms of number of peaks seen in the electropherograms. In the fourth fraction, how-

ever, no peaks are seen in the CE separation. It may be that these compounds, which elute late in the HPLC analysis, and therefore are hydrophobic, either are uncharged or are adsorbed to surfaces in the sample-transfer or separation process. The real strength of using CE to reanalyze HPLC fractions lies in the orthogonality of the separation mechanism. To fully exploit this separation power, a method is needed to couple the CE separation with mass spectrometry, either directly via CE–ES–MS or in an off-line manner running collected CE fractions by MALDI–TOF–MS. This approach has been used to characterize growth hormone tryptic peptides in a CE separation [21]. These approaches are currently under investigation, and will be reported in a future publication. Alternately, UV spectra could be used to track the elution order of a CE separation transferred from an HPLC fraction, analogously to peak tracking in HPLC peptide mapping [22]. This

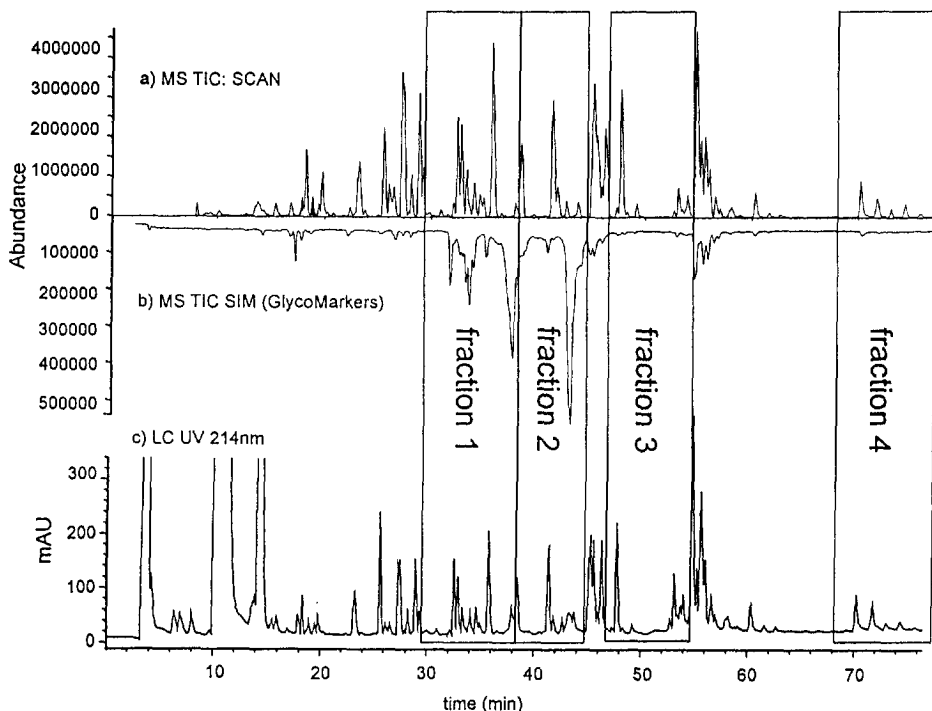


Fig. 12. Areas of HPLC fraction collection. Identification of regions from analytical separation (76 pmol). (a) Scan acquisition total-ion current (CapEx = 100 V). (b) CID SIM acquisition total-ion current (CapEx = 200 V). (c) UV at 214 nm. The actual fraction collections were done with 312 pmol injected.



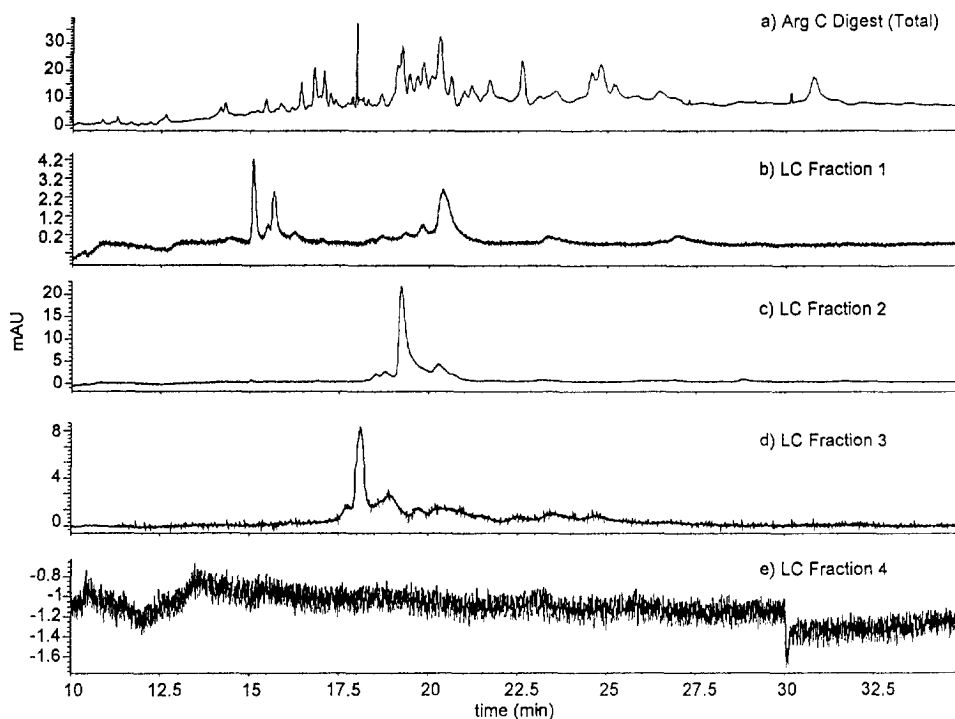


Fig. 13. HPCE of collected fractions; 30 nl injected. (a) Total Arg-C digest of DSPA $\alpha$ 1. (b) HPLC fraction 1. (c) HPLC fraction 2. (d) HPLC fraction 3. (e) HPLC fraction 4.

approach requires that the HPLC separation is already sufficiently resolved to obtain pure spectra or that pure peptide standards exist.

The four collected fractions were also analyzed by MALDI-TOF-MS, as shown in Fig. 14. This is a particularly useful combination because the sensitivity of MALDI-TOF-MS allows clear unequivocal spectra which actually exhibit a selectivity closer to HPCE than HPLC, being based on mass/charge. The orthogonality of MALDI-TOF-MS relative to HPLC generates extremely useful information. In analyzing fractions collected from the total digest, the sample complexity has been reduced sufficiently so that the MALDI-TOF-MS spectrum is a good representation of the components present in the fraction. Contrast this with the data obtained for the total digest, in which only a fraction of the components are represented by strong signals in the spectrum. If one compares the MALDI-TOF-MS result with the analysis of the digest by LC-ES-MS, there are a number of peaks in each

fraction that are present in both the electrospray and MALDI-TOF-MS data (see Table 4). A number of the ions shown in Table 4 have not yet been identified. Thus one technique reinforces peak identification based on data from the other. There are also a number of peaks that occur in either one technique or the other, but not both. Thus a more complete and accurate picture is obtained by a combination of the two.

#### Future work

It should be noted that this multidimensional approach, does not, at this stage, replace more classical techniques of protein characterization. The classical approach would include preparative isolation and purification of the intact protein and enzymatic digestion followed by collection of each of the digest fragments for complete characterization by sequencing, mass spectrometry, UV-Vis, etc. However, it seems clear that, as our abilities to integrate and interpret the large amount of data which can be produced by newer

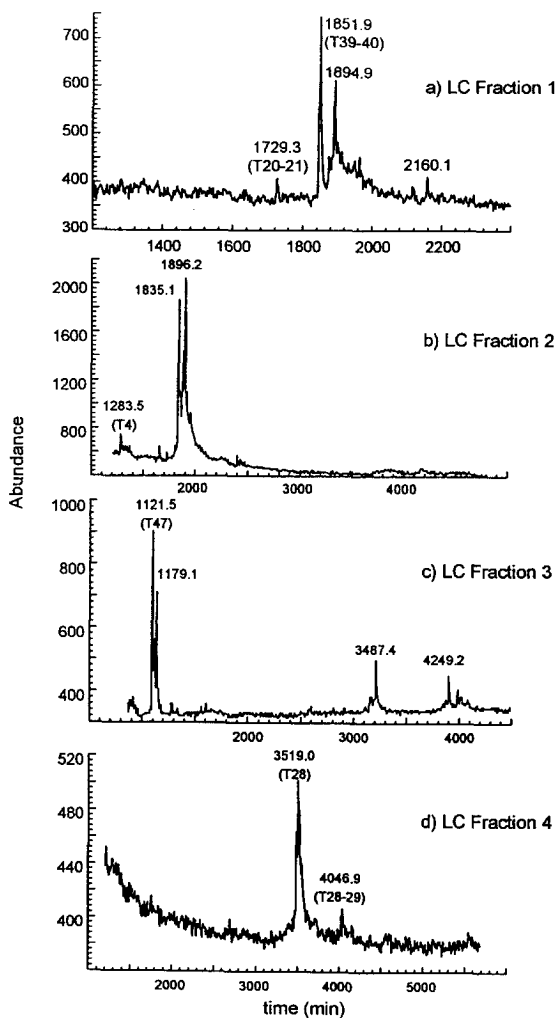


Fig. 14. MALDI-TOF-MS of collected fractions; 1  $\mu$ l of collected fractions applied. Matrix: sinapinic acid. (a) HPLC fraction 1. (b) HPLC fraction 2. (c) HPLC fraction 3. (d) HPLC fraction 4.

instrumental techniques improve, many of the more time and product consuming steps can be reduced or eliminated. This will have the overall effect of producing better data in a more timely manner.

This report represents a work in progress and there are a number of critical areas that have yet to be fully developed or exploited. Specifically:

Capillary isotachopheresis (CITP) used as a sample concentration method for HPCE is an important step in being able to exploit the

orthogonal and complimentary selectivity of HPLC and HPCE. Currently, samples eluted and collected from HPLC columns are not very well suited to analysis by HPCE in terms of concentration. Although the 'on-column' fractionation technique described above improves the situation, the ability to inject larger volumes into the HPCE capillary without sacrificing speed or resolution is needed. This situation is particularly exacerbated by the microheterogeneity of glycopeptide samples.

The on-line combination of HPCE and electrospray MS would simplify the identification of CE peaks and bring the power of MS to HPCE just as LC-ES-MS has done for HPLC. There are a number of instrumental approaches to this interface, and we are currently evaluating their use.

Although the coupling of MALDI-TOF-MS with separation techniques such as HPLC and HPCE has a great potential, as demonstrated in this work, there is a fundamental mismatch between the dynamic environment of the flow-based system and the static environment of the matrix crystal in which MALDI-TOF-MS samples are included. Sample collection from HPCE has been demonstrated in this context, and we will be evaluating this technique in the near future. Approaches for more efficiently using a greater amount of available sample for MALDI-TOF-MS also need to be developed.

#### 4. Conclusions

In this work it has been shown that HPLC, HPCE, LC-ES-MS, and MALDI-TOF-MS are highly complimentary techniques for examining glycoproteins. In a problem of this complexity, different types of data can be integrated to get a more complete characterization of the analyte. LC-ES-MS is a powerful technique for the analysis of peptide maps and shows great potential in the identification of complex regions of glycosylation. Nonetheless, more work needs to be done to improve the power of this approach. High-yield concentration steps will be required due to extensive carbohydrate heterogeneity.

Table 4  
Analysis of HPLC fractions ES-MALDI

LC fraction	ESI <i>m/z</i>	MALDI-TOF <i>m/z</i>	Sequence assignment	
1	1347.17	nd		
	1519.23	nd		
	629.21	623.1	T48[437-441]	DNMHL
	1205.3			
	745.7		T21[163-175]	FTSES CSVPV CSK
	1858.95	1851.9		
	1965.05	1966.2		
	1746.17	1729.3	T20-T21[160-175]	AGKFT SESCS VPVCS K
	1906.8	nd	T1-T2[1-16]	AYGVA CKDEI TQMTY R
	2116.77	2116.6	T38-40[331-348]	HKSSS PFYSE QLKEG HVR
	1850.92	1851.9	T39-40[333-348]	SSSPF YSEQL KEGHV R
	1876.84	1877.2		
	nd	1894.2		
	nd	2078.3		
	nd	2160.1		
2	1906.97			
	1299.2	1283.5	T4[18-27]	QESWL RPEVR
	1937.99	nd	T30-32[254-267]	KYIVH K
	1282.18	1283.5		
	1880.21	1881.3		
	966.23	nd		
	nd	1653.5		
	nd	1806.3		
	nd	1835.1		
	nd	1856		
	nd	1896.2		
	nd	1952.1		
3	1121.2	1121.5	T47[428-436]	VTNYL GWIR
	2796.14	2795.6	T33-35[270-292]	KYIVH KEFDD DTYNN DIALL QLK
	2668	2669.3	T34-35[271-292]	YIVH KEFDD DTYNN DIALL QLK
	4249.65	4249.2		
	3488.39	3487.2		
	3429	3429		
	3414.96	nd		
	nd	1136.8		
	nd	1142.2		
	nd	1163.6		
	nd	1179.1		
	nd	1327.7		
	nd	1345.9		
	nd	1387.9		
	nd	1593.3		
nd	1688.8			
nd	3031.7			
nd	3444.2			
nd	4343			
4	3518.56	3519	T28[219-248]	FLCGG ILISS CWVLT AAHCF QESYL PDQLK
	3460.31			
	3500.8	3500.8		
	4042.89	4046.9	T28-29/A21[219-253]	FLCGG ILISS CWVLT AAHCF QESYL PDQLKVV LGR
	3985.32	nd		
	3927.79	nd		
	nd	3535.8		
	nd	3630.2		
nd	4056.9			

Finally, more effective techniques are required for the integration of information from the higher-dimensional data generated by the combination of these techniques.

### Acknowledgements

The authors would like to thank Sally Swedberg and Bob Holloway at Hewlett-Packard Laboratories for help with capillary electrophoresis, Julie Sahakian-Apffel and James Kenny at Hewlett-Packard Protein Chemistry Systems for N-terminal sequencing, Steve Fischer at Hewlett-Packard Bay Analytical Operation for aid in mass spectral interpretation, Thabiso M'Timkulu and Joanne Johnson at Berlex Biosciences for carbohydrate analysis, Ray-Jen Chang and Maria Johnson at Berlex Biosciences for N-terminal sequencing, Peter Murakami and Peter Sandel at Berlex Biosciences for amino acid analysis and BaiWei Lin and Joe Traina at Berlex Biosciences for mass spectrometry.

### References

- [1] V. Ling, A.W. Guzzetta, E. Canova-Davis, J.T. Stults, W.S. Hancock, T.R. Covey and B.I. Shushan, *Anal. Chem.*, 63 (1991) 2909–2915.
- [2] A.W. Guzzetta, L.J. Basa, W.S. Hancock, B.A. Keyt and W.F. Bennet, *Anal. Chem.*, 65 (1993) 2953–2962.
- [3] S.A. Carr, M.J. Huddleston and M.F. Bean, *Protein Sci.*, 2 (1993) 183–196.
- [4] M.J. Huddleston, M.F. Bean and S.A. Carr, *Anal. Chem.*, 65 (1993) 877–884.
- [5] J.J. Conboy and J.D. Henion, *J. Am. Soc. Mass Spectrom.*, 3 (1992) 804–814.
- [6] J. Kraetschmar, B. Haendler, G. Langer, W. Boidol, P. Bringman, A. Alagon, P. Donner and W.D. Scheuning, *Gene*, 105 (1991) 229–237.
- [7] W. Witt, B. Maass, B. Baldus, M. Hildebrand, P. Donner and W.D. Scheuning, *Circulation*, 90 (1994) 421–426.
- [8] W. Witt, B. Baldus, P. Bringmann, L. Cashion, P. Donner and W.D. Scheuning, *Blood*, 79 (1992) 1213–1217.
- [9] R.M. McCormick, *Anal. Chem.*, 60 (1988) 2322.
- [10] A. Apffel, S. Fischer, G. Goldberg, P.C. Goodley and F.E. Kuhlmann, *J. Chromatogr. A*, (1995) in press.
- [11] F. Xiang and R.C. Beavis, *Rapid Commun. Mass Spectrom.*, 8 (1994) 199.
- [12] P. Oroszlan, S. Wicar, G. Teshima, S.-L. Wu, W.S. Hancock and B.L. Karger, *Anal. Chem.*, 64 (1992) 1623–1631.
- [13] J.B. Fenn, M. Mann, C.K. Meng, S.F. Wong and C.M. Whitehouse, *Science*, 246 (1989) 64–71.
- [14] T. M'Timkulu, unpublished results.
- [15] A.W. Guzzetta and W.S. Hancock, *Recent Advances in Tryptic Mapping*, CRC Series in Biotechnology, CRC Press, Boca Raton, FL, 1994, in press.
- [16] M.W. Spellman, L.J. Basa, C.K. Leonard, J.A. Chakel, J.V. O'Connor, S.W. Wilson and H. van Halbeek, *J. Biol. Chem.*, 264 (1989) 14100–14111.
- [17] M.M. Bushey and J.W. Jorgenson, *Anal. Chem.*, 62 (1990) 978–984.
- [18] R.L. Chein and D.S. Burgi, *J. Chromatogr.*, 559 (1991) 141–152.
- [19] F.E.P. Mikkers, Thesis, Eindhoven University, Eindhoven, 1980.
- [20] F. Foret, E. Szoko and B.L. Karger, *J. Chromatogr.*, 608 (1992) 3–12.
- [21] M. Herold and S.-L. Wu, *LC·GC*, 12 (1994) 531–533.
- [22] H.-J.P. Sievert, S.-L. Wu, R. Chloupek and W.S. Hancock, *J. Chromatogr.*, 499 (1990) 221–234.